Supplementary Online Content

Ku CA, Hull S, Arno G, et al. Detailed clinical phenotype and molecular genetic findings in *CLN3*-associated isolated retinal degeneration. *JAMA Ophthalmol*. Published online May 25, 2017. doi:10.1001/jamaophthalmol.2017.1401

This supplementary material has been provided by the authors to give readers additional information about their work.

eTable. Functional prediction of *CLN3* mutations associated with isolated retinal degeneration

Allele 1	Allele 2	Associated Phenotype	Prediction platform, pathogenicity score
c.125+1G>C (Intron 2-3 spl)	c.1213C>T (R405W)	arRP[1]	BDGP, 0.91
c.125+5G>A (Intron 2-3 spl)	c.424delG (Val142Leufs*39)	JNCL[2]	
c.375-3C>G (Intron 5-6 spl) *	1.02-kb del	Early arRCD	BDGP, 0.94
c.391A>G (S131R)	c.883G>A (E295K)	arCORD[1]	PolyPhen2, 0.91 (D)
c.461-3C>G (Intron 6-7 spl) *	1.02-kb del	arRCD	BDGP, 0.99
c.461-13G>C (Intron 6-7 spl)	1.02-kb del	JNCL[3]	
c.461-1G>C (Intron 6-7 spl)	1.02-kb del	JNCL[2]	
c.565G>C (G189R)	c.565G>C (G189R)	arRP[1]	PolyPhen2, 1.0 (D)
c.565G>C (G189R)	1.02-kb del	JNCL[2]	
c.597C>A (Y199X)	c.597C>A (Y199X)	LCA (Age 6)[5]	(truncation)
c.597C>A (Y199X)	c.597C>A (Y199X)	Protracted JNCL[6]	
c.837+5G>A (Intron 10-11 spl) *	1.02-kb del	arRCD	BDGP, 0.96
c.853A>G (I285V) *	1.02-kb del	Early arRCD	PolyPhen2, 0.0 (B)
c.868G>T (V290L)	c.966C>G (Y322X)	arRP[1]	PolyPhen2, 0.03 (B)
c.883G>T (E295X)	c.917T>A (L306H) *	Early arRCD	(truncation)
c.883G>T (E295X)	unspecified	JNCL (?)[4]	
c.883G>A, (E295K)	c.391A>G (S131R)	arCORD[1]	PolyPhen2, 0.99 (D)
c.883G>A, (E295K)	1.02-kb del	Protracted JNCL[3]	
c.883G>A, (E295K)	1.02-kb del	Protracted JNCL[7]	
c.883G>A, (E295K)	1.02-kb del	Protracted JNCL[8]	
c.917T>A (L306H) *	c.883G>T (E295X)	arRCD	PolyPhen2, 1.0 (D)
c.966C>G (Y322X)	c.868G>T (V290L)	arRP[1]	(truncation)
c.988G>A (V330I) *	1.02-kb del	arRCD	PolyPhen2, 1.0 (D)
c.988G>T (V330F)	1.02-kb del	JNCL[3]	PolyPhen2, 1.0 (D)
c.1213C>T (R405W)	1.02-kb del	Early arRCD	PolyPhen2, 1.0 (D)
c.1213C>T (R405W)	c.1213C>T (R405W)	arRCD	
c.1213C>T (R405W)	c.1213C>T (R405W)	arRP[1]	
c.1213C>T (R405W)	c.125+1G>C	arRP[1]	

Predicted functional effects and associated phenotype of mutations. Abbreviations: spl, splice; BDGP, Berkeley Drosophila Genome Project; (B) benign; (D) damaging; (?) unspecified JNCL phenotype (classic or protracted); gray highlight, mutations associated with isolated retinal degeneration; *novel mutations reported in this study.

References for eTable.

1 Wang F, Wang H, Tuan HF, et al. Next generation sequencing-based molecular diagnosis of retinitis pigmentosa: identification of a novel genotype-phenotype correlation and clinical refinements. Hum Genet. 2014;133(3):331-345.
2 Kousi M, Lehesjoki AE, Mole SE. Update of the mutation spectrum and clinical correlations of over 360 mutations in eight genes that underlie the neuronal ceroid lipofuscinoses. Hum Mutat. 2012;33(1):42-63.
3 Munroe PB, Mitchison HM, O'Rawe AM, et al. Spectrum of mutations in the Batten disease gene, CLN3. Am J Hum Genet. 1997;61(2):310-316.
4 London UC. NCL Resource - A gateway for Batten disease: 2015, 2016,
5 Wang X, Wang H, Sun V, et al. Comprehensive molecular diagnosis of 179 Leber congenital amaurosis and juvenile retinitis pigmentosa patients by targeted next generation sequencing. J Med Genet. 2013;50(10):674-688.
6 Sarpong A, Schottmann G, Ruther K, et al. Protracted course of juvenile ceroid lipofuscinosis associated with a novel CLN3 mutation (p.Y199X). Clin Genet. 2009;76(1):38-45.
7 Wisniewski KE, Zhong N, Kaczmarski W, et al. Compound heterozygous genotype is associated with protracted juvenile neuronal ceroid lipofuscinosis. Ann Neurol. 1998;43(1):106-110.
8 Zhong N, Wisniewski KE, Kaczmarski AL, et al. Molecular screening of Batten disease: identification of a missense mutation (E295K) in the CLN3 gene. Hum Genet. 1998;102(1):57-62.

eFigure 1. Pedigrees and mutation segregation in 5 families for 6 patients

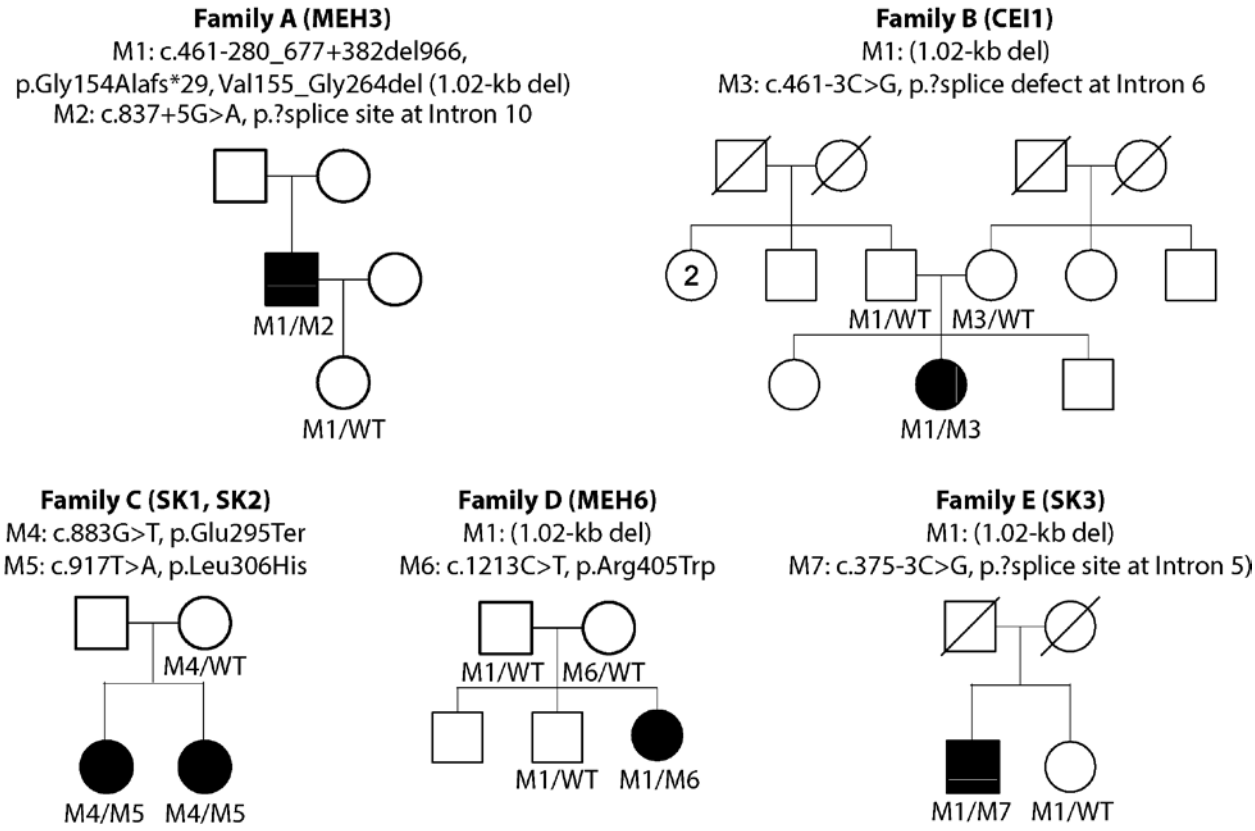

Abbreviations: Circles, female individuals; squares, male individuals; filled symbols, affected; hollow symbols, unaffected; M, mutation allele; WT, wild type allele.

eFigure 2. Supplementary full-field electroretinograms

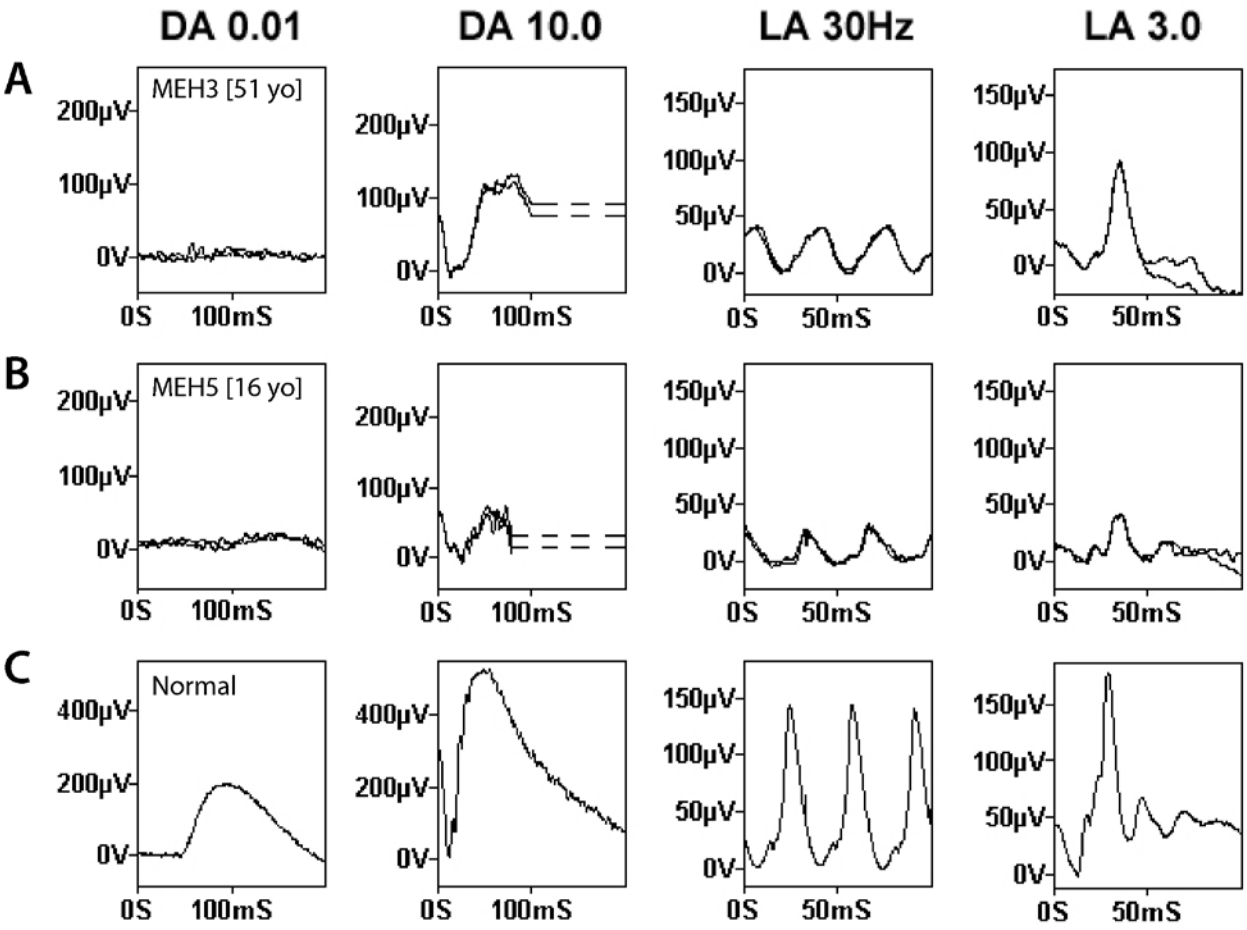

ffERG responses of (A) MEH3, (B) MEH5, and (C) normal unaffected control, under dim scotopic (DA 0.01), bright scotopic (DA 10.0), photopic flicker (LA 30 Hz), and photopic single flash (LA 3.0). Brackets indicate age of ERG testing. Abbreviations: DA, dark-adapted; LA, light-adapted; mS, milliseconds; µV, microvolts.

eFigure 3. Multifocal electroretinography of patients with late-onset retinal degeneration who retain residual full-field cone responses

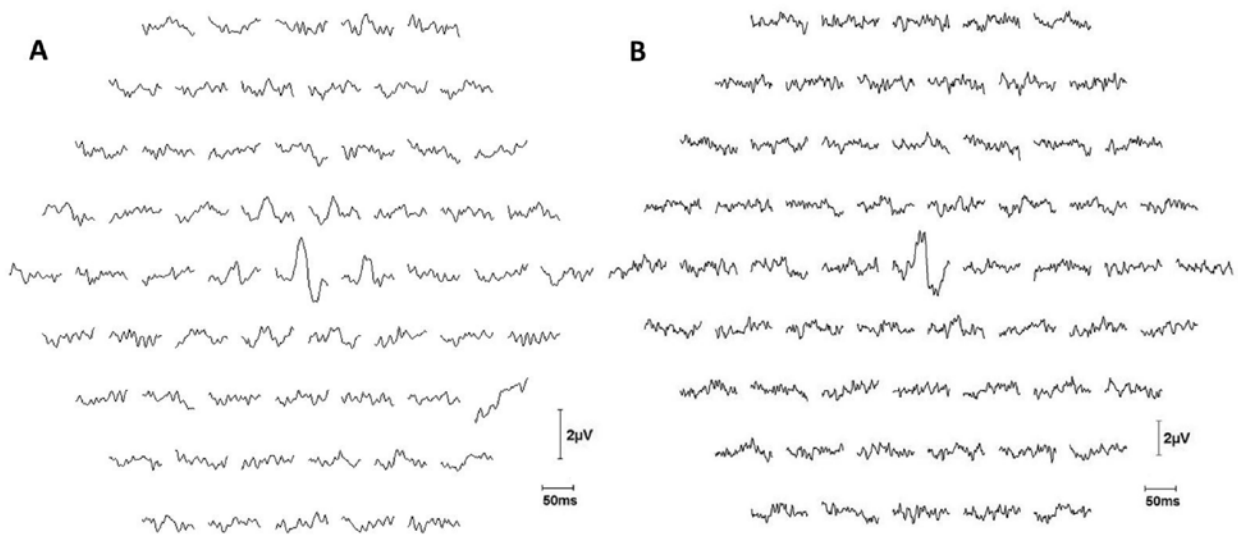

mfERGs demonstrating residual central responses with decreased paracentral responses in the macula in (A) patient MEH1, and (B) patient MEH4.

eFigure 4. Evaluation of the effect of intronic mutation c.461-3C>G on *CLN3* transcript level and autofluorescent phenotype

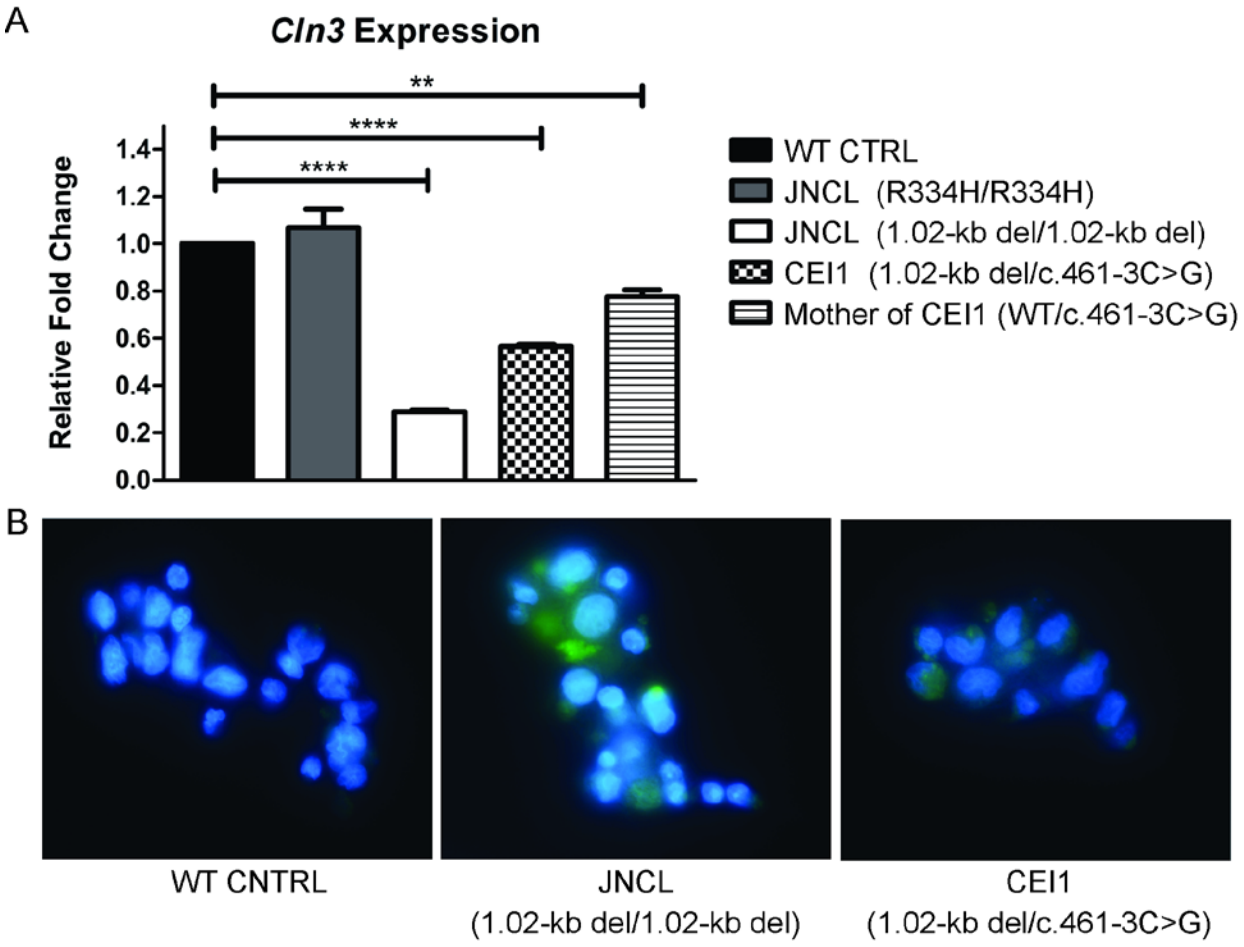

(A) CLN3 transcript levels in patient CEI1 (1.02-kb deletion/c.461-3C>G) is abnormally low compared to wild type controls (WT CTRL), although not decreased to the level of homozygous 1.02-kb deletions. Transcript levels from homozygous R334H missense mutations is shown as another control reference; this homozygous mutation has been previously shown to have transcript levels comparable to wild type despite causing a JNCL phenotype (Miller et al., 2013, *Hum Mol Genet*, 22(13):2723-2734). Transcript levels in the maternal intronic carrier (WT/c.461-3C>G), although greater than her compound heterozygous daughter, is not restored to wild type levels, suggesting that this intronic mutation may lead to abnormal transcription. *CLN3* transcript abundance was measured as previously reported (Miller et al., 2013). Briefly, lymphoblast cell lines were processed for RNA extraction and purification (#AS1270, Promega). RNA quality was evaluated using an Epoch Microplate Spectrophotometer prior to reverse transcription of 1 µg of RNA into cDNA (#A5000, Promega). Relative *CLN3* transcript abundance was measured using a *CLN3* gene expression assay kit (#Hs01029229_g1, Life Technologies) with normalization to *GAPDH* transcript abundance (#4333764F, Life Technologies). Relative fold expression of triplicate samples was calculated using ΔΔCT.
(B) Lymphoblasts in CEI1 showed present but less autofluorescent deposition than in *CLN3*-JNCL patients with a homozygous 1.02-kb deletion, who show characteristic high autofluorescence from lipofuscin accumulation.

eFigure 5. Patients show electroretinography responses with reduced b-wave to a-wave ratio under scotopic conditions

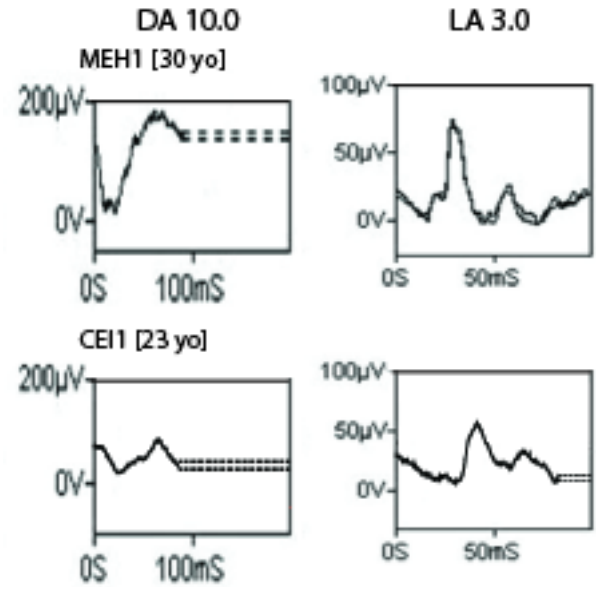

ffERG responses under scotopic dark-adapted (DA 10.0) conditions and photopic light-adapted conditions (LA 3.0) in patient MEH1 (top row) and CEI1 (bottom row). Light-adapted responses did not demonstrate abnormal b- to a- ratios.